A&A manuscript no.
(will be inserted by hand later)

Your thesaurus codes are:
06 (08.15.1; 08.09.2; 03.20.8)

ASTRONOMY AND ASTROPHYSICS
September 8, 1999

Evidence for global pressure oscillations on Procyon *

M. Martić[1], J. Schmitt[1], J.-C. Lebrun[1], C. Barban[2], P. Connes[1], F. Bouchy[1], E. Michel[2], A. Baglin[3], T. Appourchaux[4] and J.-L. Bertaux[1]

[1] Service d'Aéronomie du CNRS, BP No 3, 91371 Verrières le Buisson, France
[2] Observatoire de Paris, DASGAL, CNRS UMR 8633, 92195 Meudon, France
[3] Observatoire de Paris, DESPA, CNRS UMR 8632, 92195 Meudon, France
[4] Space Science Departement of ESA, ESTEC, NL-2200 AG Noordwijk

Received ;Accepted date

Abstract. Precise Doppler measurements of the star Procyon (α CMi, HR 2943) have been obtained with the ELODIE fiber-fed cross-dispersed echelle spectrograph on the 1.93 m telescope at Observatoire de Haute Provence. Here, we present the analysis of data from 10 days observing run carried out in November 1998. We detect significant excess in the power between 0.5–1.5 mHz in the periodograms of the time series of mean Doppler shifts. Observations of η Cas made with the same instrument during the same time interval and in almost identical night conditions show a flat spectrum in this frequency range, indicating that the excess of Doppler signal seen on Procyon is of stellar origin. When data from the whole run are jointly analyzed, a period analysis places an upper limit of 0.50–0.60 ms^{-1} for the amplitude of oscillations, while the frequency cutoff is around 1.5 mHz. The power evidently drops near 0.55 and 1.5 mHz on the average of unfiltered power spectra of individual nights, which is consistent with the expected p-mode oscillation properties for Procyon. Several equispaced peaks in frequency are recurrent in the power spectra of two independent segments of 4 and 3 contiguous nights; the most probable frequency spacing seems to be 55 μHz. In conclusion, we now have an instrument set-up which is sufficiently stable and fast to be used for a multi-site campaign involving instruments with comparable velocity precisions, to detect the oscillation modes of sun-like stars.

Key words: stars: oscillations – stars: individual: Procyon – techniques: spectroscopic

1. Introduction

The Procyon binary system consists of an F5 IV-V primary and a white dwarf secondary with a 40 year orbit. Procyon A is an apparently ordinary object but of great interest to Doppler seismology of solar-like stars. It is the brightest northern hemisphere candidate with well-determined characteristics, which simplifies the interpretation of asteroseismological results. There has been a long standing discrepancy between astrometric mass determination of Procyon (1.75 $M_\odot$) by Irwin et al. (1992) and astrophysical mass (1.5 $M_\odot$) required by stellar evolution modelling (e.g. Guenther and Demarque, 1993) to reproduce Procyon's observed luminosity and temperature. This has stressed the importance of an unambiguous detection of the oscillations in order to constrain the stellar-interior model. The problem of Procyon's mass has posed a challenging task to asteroseismology to discriminate between these two values for the mass but, on the other hand it did not help to confirm different new instrumental and reduction methods and especially mode identification.

For example, Gelly et al. (1986) using a resonance cell spectrometer, reported the detection of solar-like modes on Procyon with a mean first-order half spacing $0.5\,\Delta\nu_0$ of 39.7 μHz, while Brown et al. (1991) found 35.5 μHz when observing with the FOE spectrograph. Other attempts were made with a Fabry-Perot interferometer (Ando et al., 1988), and magneto-optical filter (Innis et al. 1991, Bedford et al. 1995).

Finally, the solution of this mass discrepancy problem came from new astrometric measurements based on Wide Field Planetary Camera Images (WFPC2) by Girard et al. (1996) who obtained a mass of $1.470 \pm 0.045 M_\odot$ for Procyon A, which agrees well with the prediction of previous models. Chaboyer et al. (1998) calculated a new grid of stellar evolution models for Procyon A, based on the revised astrometric mass, and predict the large separation to be between 52.91 μHz and 55.47 μHz. They claimed that measuring the large separation with a precision of at least 1 μHz should allow to determine wether Procyon is still on the main sequence or in a shell hydrogen burning stage. However, such a precise determination of the large separation is difficult to obtain from single site observations which are limited by the day-night cycle. This is in favor of

Send offprint requests to: M. Martić

* Based on observations obtained at the Observatoire de Haute-Provence (CNRS, France)

Correspondence to: milena@aerov.jussieu.fr

Table 1. Observational log(UT time)

	Procyon					η Cas			
Date	Start	End	Nb spectra	$\sigma(ms^{-1})$	Date	Start	End	Nb spectra	$\sigma(\mathrm{ms}^{-1})$
98/11/07	00.00	06:11	307	4.17	98/11/07	18:05	23:32	193	1.99
98/11/08	23:48	06:17	322	4.55	98/11/08	18:03	23:19	187	2.46
98/11/10	00:33	04:11	151	4.01	98/11/09	17:31	23:19	203	2.99
98/11/10	23:45	06:15	230	5.01	98/11/10	17:45	22:58	185	3.95
98/11/11	23:37	01:41	91	—	98/11/11	17:53	23:14	190	
98/11/12	23:29	05:16	248	3.89	98/11/12				
98/11/14	23:29	06:07	291	3.31	98/11/14				
98/11/15	23:38	06:21	294	3.37	98/11/15	17:49	23:06	187	
98/11/16	23:24	07:06	338	2.69*	98/11/16	17:56	22:43	170	

* A few bad spectra eliminated

multi-site observational campaigns involving sites well distributed in longitude and using instruments having comparable photometric or spectroscopic precision. The best time-series coverage (156 hours) was obtained thus far by Gilliland et al. (1993) using a global network of several 4-m telescopes to search for oscillations in stars of the cluster M67. These observations tentatively approached the limit of differential CCD photometry but no solar-like oscillations were unambiguously detected. Other attempts were made to detect small amplitude p-mode oscillations on very few possible bright solar or near-solar type star candidates (Gelly et al. 1986, Brown & Gilliland 1990, Pottasch et al. 1992, Edmonds & Cram 1995, Kjeldsen et al. 1995 etc.), but none of them were conclusive or confirmed by an independent team of observers.

Recent advances in echelle spectroscopy have led to important improvements in the precision of radial velocity measurements (Brown, 1998). Mayor & Queloz (1995) succeeded in detecting the first exo-planet around the nearby star 51 Peg using a new ELODIE fiber-fed echelle spectrograph at Observatoire de Haute Provence (OHP). Our first observing runs (Connes et al. 1996) were dedicated to evaluate the suitability of the ELODIE spectrograph for asteroseismology. ELODIE was designed for precise Doppler measurements, but the whole system (e.g., guiding camera, shutter, data reduction etc.) was not tested for the use in a rapid cadence necessary for the detection of oscillations on stars similar to the Sun.

Over the past three years, the instrument and observing runs were optimized to measure the fluctuations in radial velocities for a sample of bright stars that are likely to undergo solar-like oscillations. A more extensive discussion of the actual instrument performances tested on these stars, mainly on those which have the narrowest spectra and excellent photon rates, will be presented in a subsequent paper. Here, we report the observations of Procyon A and η Cas (HR219). The primary target, Procyon, has a higher expected amplitude of oscillations in the low frequency domain, compared to the fainter star η Cas. However, as a G-type solar analog star, η Cas has expected oscillations in a higher frequency band than Procyon, at a place where instrumental noise is lower.

2. Observations

The observations were carried out using the ELODIE echelle spectrograph which was newly installed on the 1.93 m OHP Telescope. A full design of the spectrograph is explained in Baranne et al. (1996, hereafter Paper 1). The ELODIE spectrograph is fed from the Cassegrain focus using 100μ optical fibers. The fibers avoid light losses, and improve the uniformity of illumination in the spectrograph (e.g. Connes 1978). Our first results (Connes et al. 1996) on a bright star ψ UMa HR4335 (V=3.0, K1III) showed some fast fluctuations coming from imperfect stellar-beam scrambling by the optical fibers. Last year, a significant improvement was obtained by introducing a double-scrambler (built by D. Kohler at OHP) on the stellar fiber path, which reduces the spurious line shifts due to changes in spectrograph illumination. In order to monitor the spectrograph calibration variations, the reference fiber is illuminated, during stellar exposures in regular ELODIE operation, by a Thorium-Argon lamp. In our configuration we introduced in the sky-hole, the channelled spectrum obtained with white light through a fixed (ZERODUR) Fabry-Perot (FP) interferometer, which insures, by using the second optical fiber, the condition of almost identical optical path crossed by the stellar beam and FP beam. The comb of fringes from the Fabry-Perot etalon is exposed on the detector simultaneously with the stellar spectrum. The FP etalon has a thickness of 6 mm and fringe spacing of $72\,\mu$m (3 pixels) and it is temperature-controlled to a precision of 0.01 K.

To check various sources of errors in spectrograph operation like the variations due to the thermal relaxation, air pressure variations and CCD cooling, we made simultaneous recordings of FP/FP spectra on both fibers.

We will show in the following sections that we are able to achieve a similar or better accuracy to that of the absorption cell instruments. Actually, the Absolute Accelerometry technique proposed by Connes (1985) and observations described here do not suffer from the limitation of introducing a gas cell in the beam which increases the photon-noise radial velocity limit.

The optical layout, as explained in Paper 1, allows to record in one single exposure a wavelength domain from 390.6 to 681.1 nm at a resolution of $R \sim 42000$. The 67 orders are recorded, each covering about 52.5 nm and with an overlap of about 10 nm between adjacent orders, on a Tk 1024 CCD with 24 μm pixels. A rapid cadence for our observations is achieved by a parallel readout (7.5 microsec/pixel) of the two halves of the CCD with a read-out noise of 4.2 e^- which is insignificant for the high levels of the illumination we used. The CCD detector is currently maintained at 183 K operating temperature during observing runs. It needs twice-daily filling of a liquid-nitrogen dewar which introduces an important thermal shock but of short duration at the beginning and at the end of long observing runs.

A total of 10 nights of OHP 1.93 m telescope time were allocated in November 1998 for the observations reported here. In addition to our primary target, Procyon, we also observed the star η Cas for four hours at the beginning of each night. A journal of the observations is given in Table 1. We took sequences of about 40 s exposures, which with detector readout time and transfer of images yielded an almost regular interval between exposures averaging 90 s. In our run we did not use atmospheric differential correctors since setting up and checking the corrector position is rather time consuming. The Doppler rms shown in the last column of the Table 1 applies to the time series of the data after all reductions described below have been carried out.

3. Data Reduction

The reduction was carried out using a modified standard ELODIE data analysis package to extract the echelle spectra from row CCD (1024x1024) frames which where previously corrected pixel by pixel by subtracting the bias. The position of the orders on the detector is obtained by illuminating the fibers by a tungsten lamp. The geometrical definition and extraction of the orders based on Horn's (1986) algorithm are explained in detail in Paper 1. In our configuration, the result of this process produces for each CCD exposure a set of stellar and Fabry-Perot spectra interleaved into 67 echelle orders falling on the frame. Fig. 1 shows some typical extracted Procyon and Fabry-Perot spectra. We used neutral density filters to maintain consistent exposure levels from the FP beam for the different exposure times depending on weather conditions and star signal. The advantage of using the closely-spaced channelled spectrum from a fixed FP is that it gives the best possible reference even for very short exposure times of bright stars.

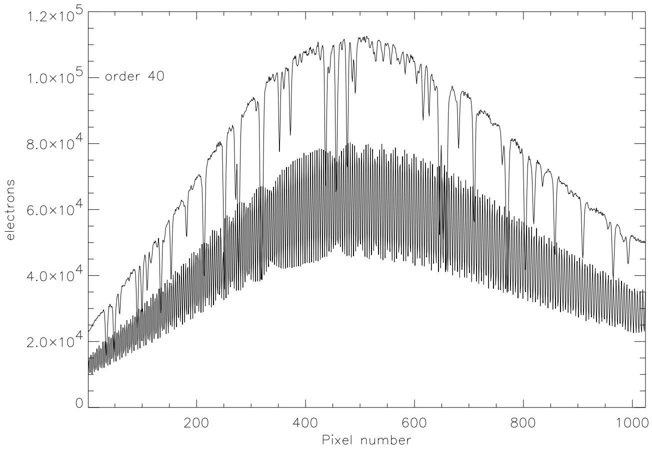

Fig. 1. Examples of stellar and Fabry-Perot spectra from a single order. The wavelength range is 519-524 nm.

The main modification of regular ELODIE software consisted of its adaptation to the observing run in order to obtain long uninterrupted sequences with high temporal resolution. Actually, not just during the development phase of this program but also during the observations we found it extremely useful to have real time reduction and display of the Doppler shifts and power spectra at the end of each exposure. This allowed us to rapidly correct for, when possible, problems concerning CCD output, guiding errors, etc. The extraction of the 67 spectra for both star and FP and a computation of velocity shifts with our Sun Sparc station (with two fast processors) took less than 40 s which is of the order of the CCD readout time. The standard radial velocity computation by a cross-correlation algorithm was replaced by our own algorithm based on a method explained in detail in Connes (1985).

The upper part of Fig. 2 shows the simultaneous time series of the FP and stellar mean Doppler shifts and telescope motion relative to the solar system barycentre for one night. The echelle orders were averaged by weighting each order with the inverse square of its time-series rms. Orders 1 to 9 were not taken in the resulting mean shift because of poor signal. The lower part of the Fig. 2 shows the stellar shift for the same night after subtracting the instrumental drift (FP time sequence) and correction for earth's motion. The rms residual is $\sim 3\,\mathrm{ms}^{-1}$ as compared roughly to $1\,\mathrm{ms}^{-1}$ expected from photon noise alone. Note that after wavelength calibration, the velocity of $100\,\mathrm{ms}^{-1}$ corresponds to a 0.0316 pixel displacement. The accurate wavelength scale is obtained using a Thorium-Argon lamp; but this calibration is not necessary if we recall a useful property of echelle spectra, that in the spectrograph image plane the ratio $\Delta\lambda/\lambda\ 1/dx$ is very nearly a constant, independent of the order or of the position within orders.

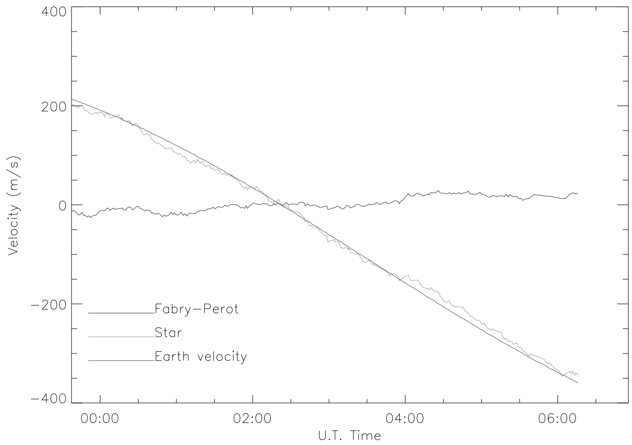

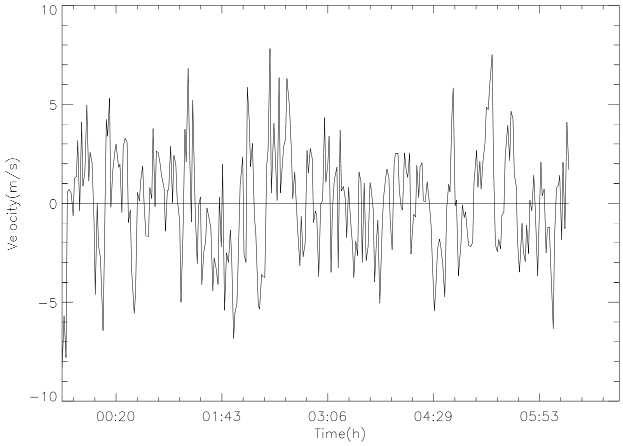

Fig. 2. Time series of the mean Doppler shifts. Top panel : Doppler shift of Procyon superposed to the radial earth velocity and instrumental shift as measured by the Fabry-Perot (FP) spectrum. Bottom panel : Residual averaged Doppler shift after the correction for Earth's motion and subtraction of the FP shift.

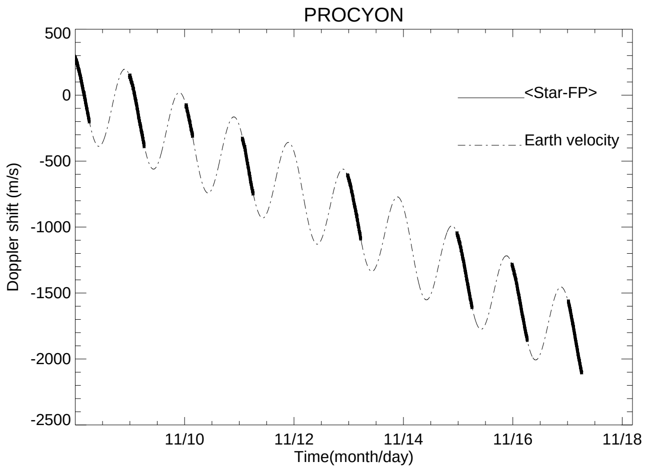

Fig. 3. Residual mean Doppler shift of Procyon superposed to the diurnal and orbital components of the relative earth velocity for the whole observing run.

As a result Brown (1995) argues that the Doppler shifts appear as translations of the entire spectrum in the direction parallel to the dispersion with no stretching or deformation of the spectra. In our case, we computed the velocity shift taking into account the Doppler stretch but, we found very small differences compared to the constant case.

Fig. 3 illustrates the result of overall reduction on Procyon data from the whole 10 nights run. Individual bad points (clouds, non-corrected cosmic rays) were replaced with linearly predicted points or simply eliminated by comparing the difference of two successive spectra, when the shift is calculated. Subtraction of the scattered straylight, since the orders are very close, was achieved by using respectively, star only or FP only exposures for reference. We verified that the scaling law "average intensity on one fiber/average scattered light on the other fiber" is roughly preserved. The effect of the approximate correction of the straylight contamination in the average is small since the first low S/N orders were not used in averaging. The same is true for higher orders affected by the telluric lines. They were not systematically included in the computation of the mean shift. Nevertheless, we obtained a telluric water vapor template by observing the nearly featureless spectrum of a rapidly rotating B star, as suggested by Young & Rottler (1992). For the orders contaminated by the telluric lines, a mask was constructed and residual lines were used to calculate the shift. We made this effort in order to use, as much as possible, the broad wavelength coverage provided by ELODIE echelle spectrograph.

It is worth noting that the photon-noise limited Doppler sensitivity can be approached only using a very large number of narrow lines from stellar spectra. For η Cas, whose spectrum has a high quality Q factor similar to the Sun (Q $\sim$ proportional to the number, depth and finesse of the spectral lines, see Connes 1985) we obtained for one order Qmax=12137. This is to be compared with the Qmax=14179 for a spectrum of the Sun obtained during the daytime runs in scattered light. The Qmax for the Fabry-Perot spectra is 40000 and the photon noise limit obtained from the whole spectral range in 40 s integration, is of the order of 0.2 ms^{-1}. For Procyon (Qmax=8672), we calculated, for an average S/N in a single exposure of 40 s a photon noise equal to 0.8 ms^{-1}. For one hour of our best run, the measured radial velocity deviation is approximately twice the photon noise limit.

4. Stellar power spectra analysis

We used the Lomb-Scargle (LS) modified algorithm (Lomb 1976, Scargle 1982) for unevenly spaced data to compute the power spectra of the Doppler shift time series de-

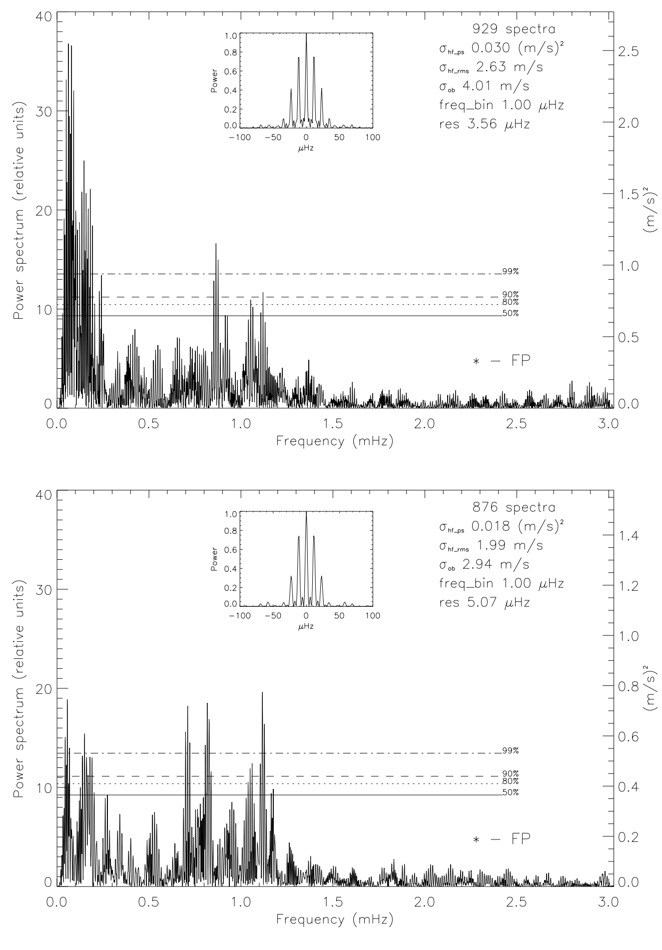

Fig. 4. Power spectra of the Doppler shift for Procyon, computed with 1μHz resolution. The mark "*-FP" indicates that the instrumental drift measured by simultaneous Fabry-Perot (FP) recordings was subtracted from the star (*) Doppler shift (see text). Top panel : Power spectrum of the four first nights (Nov 7-10, 1998). Bottom panel : Power spectrum of the three last nights (Nov 14-16, 1998). The horizontal dashed lines indicates the amplitude of several peaks having a "true alarm probability" of $\geq$50%. The inset shows the power spectrum of the window function for a signal amplitude of $1\,\mathrm{ms}^{-1}$ and the same sampling rate as the observations.

scribed in Table 1. The sampling rate in the individual nights was almost constant (90 s) but the window function of the entire run was complicated by two missing nights (or large gaps of 42 hours) due to the weather conditions. Therefore, we first separated the Procyon data into two independent sets of Doppler shift time series : the first one results from the concatenation of the four adjacent nights of observation, the second one from the three last nights.

Fig. 4 shows the LS periodograms, at a frequency resolution of $1\,\mu$Hz, of the first sequence and the second one separated about 78 hours from the first. The window function plotted in the inset shows sidelobes whose frequency separation is about 1/day=11.57 μHz. The two power spectra show an excess power around 1 mHz with a few common peaks in the 0.6–1.5 mHz band where p-mode oscillations are expected to occur. The sharp cut-off below 50 μHz is due to the linear detrending, but no other high-pass filtering operation was used. The power at frequencies up to 0.3 mHz is rather low which indicates the excellent elimination of the instrument instabilities by simultaneous FP recordings. The rms scatter σ_{rms} (σ_{ob} in Fig. 4) is greater for the first sequence of four nights ($4.01\,\mathrm{ms}^{-1}$) than for the second sequence of three nights ($2.94\,\mathrm{ms}^{-1}$). The mean white noise level in the power spectrum $\sigma_{\mathrm{hf\_ps}}$ within the frequency interval 2–5 mHz is respectively $0.03\,(\mathrm{ms}^{-1})^2$ and $0.018\,(\mathrm{ms}^{-1})^2$ for the first and second data set (see Fig. 4).

In order to estimate the statistical significance of the peaks in 0.6–1.5 mHz frequency range, we used the statistical properties of the LS periodogram. According to the method of Horne - Baliunas (1986), we calculated a few levels of power corresponding to a few values of the quantity (1-F) where F is the "false alarm probability". Four peaks have an amplitude equal or higher than the level probability of 80% (see Fig. 4) and may result from a genuine signal particularly for the last sequence which has the best signal to noise ratio. A positive result is also obtained when we calculate according to Hoyng (1976) the relative error of individual peaks. This relative error expressed by :

$$\sigma(\nu)/P(\nu) \approx (2x - x^2)^{1/2} \text{ where } x = \sigma_{\mathrm{hf\_ps}}/P(\nu)$$

gives the probability that data are pure noise. For two common peaks at ~1.120 mHz in both sequences, we estimated respectively a relative error of 26 % and 21 %.

In order to calculate the amplitude of the signals suspected to be the oscillation modes of Procyon, we used the following formulae (Kjeldsen & Bedding 1995) :

$$(A_{\mathrm{osc}})^2 = (A_1)^2 - (8.7 \pm 2.3)\sigma^2_{\mathrm{amp}}$$

where A_1 is the amplitude of the strongest peak, σ_{amp} is the mean noise level in the amplitude spectrum and A_{osc} is the searched "true" amplitude. If we assume only a gaussian white noise around 1 mHz, we have $\sigma^2_{\mathrm{amp}} = \pi\sigma_{\mathrm{hf\_ps}}/4$. Using the statistical values written on the graphs, we estimate the amplitude of the peak at frequency $\nu_{\max} = 1.12\,\mathrm{mHz}$ to about $0.75\,\mathrm{ms}^{-1}$ for the two sequences.

The difference of power in other large peaks of two data sets might be explained by constructive interference with noise. We did not apply a high-pass filter on the individual time sequences in order not to artificially create or modify the shape of the hump of power.

The individual peaks can also be examined by simple visual inspection of the oscillation frequencies on the single-night spectra. Several nights of data on Procyon show the repeatability of the structure (see Fig. 5) in the power spectrum. The excess of power and few common peaks present in adjacent nights indicate the possible detection of coherent oscillations.

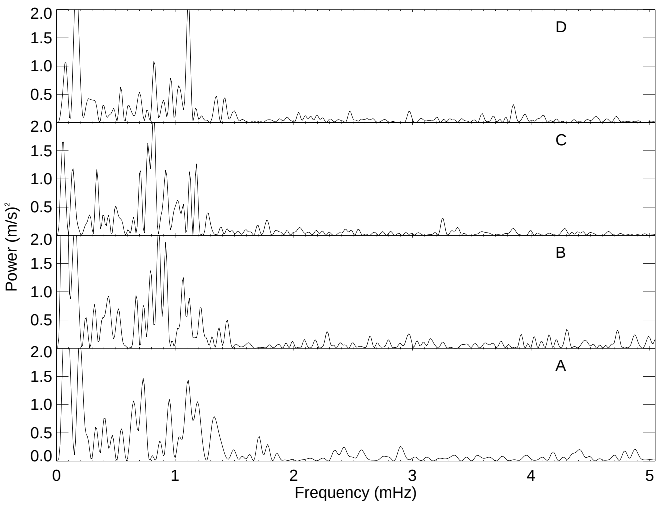

Fig. 5. Power spectra of the Doppler shift for Procyon computed for four individual nights of observations in 1998. The spectra are shown at a frequency resolution of 10 μHz.
A Power spectrum, 7-8 Nov. **B** Power spectrum, 8-9 Nov. **C** Power spectrum, 14-15 Nov. **D** Power spectrum, 15-16 Nov.

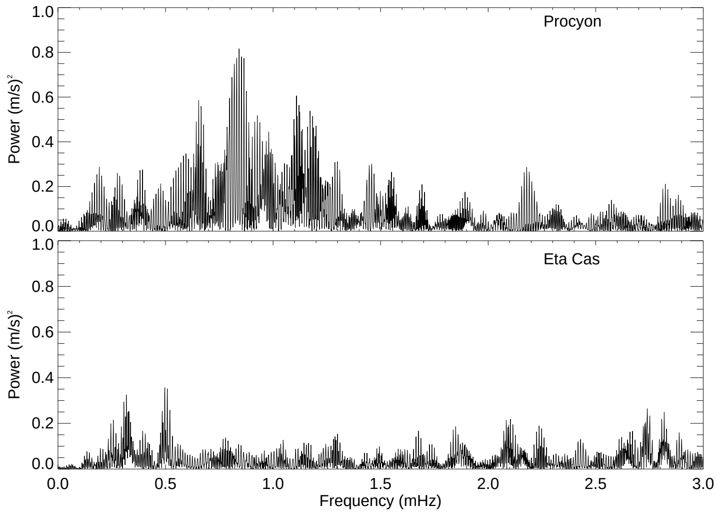

Fig. 7. Power spectra of the Doppler shift for Procyon and η Cas computed from the first four nights of the observations. The data of Procyon were cut in order to have the same number of spectra by night for the comparision. The low frequency contribution has been slightly filtered out.

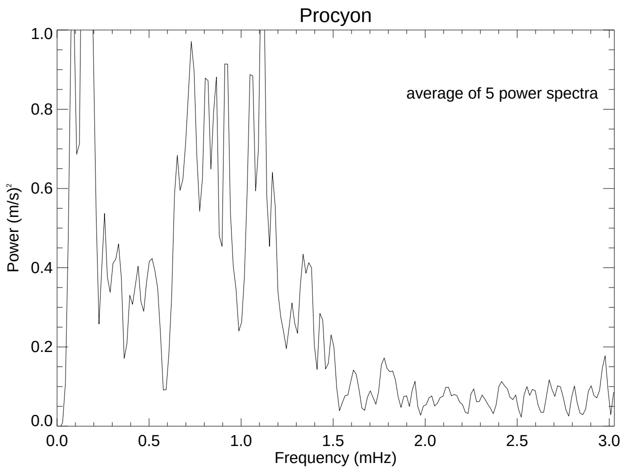

Fig. 6. Average of power spectra of the Doppler shift measurements for Procyon over 5 best nights of observations in 1998.

Another test for the existence of periodic signal in the power spectrum is to compute the average power spectrum. The hump of excess power between 0.5 and 1.5 mHz is always present when we calculate a trivial average by adding several power spectra of the Doppler shift of individual nights of observations (see Fig. 6). An obvious low-frequency cutoff, already visible in the best individual nights, appears at about 0.55 mHz.

In addition, the power spectra of Procyon and η Cas (see Fig. 7) derived from the same number of Doppler shift measurements obtained during the same 4 nights show clearly the existence of an excess of power on Procyon within the frequency range 0.55–1.5 mHz compared to η Cas. The mean high frequency noise level in the power spectrum, equal for the two series of data, is about 0.035 $(\mathrm{ms}^{-1})^2$. Since η Cas was observed only for about four hours at the beginning of each night, the length of the sequence was too short to allow to search for the p-modes on this solar analog star. Note however, that with this noise level in 5-min band and longer runs, we can expect to detect in the future the oscillations on η Cas.

Figure 8 (left top panel) shows the power spectrum of the complete data set for Procyon from 8 nights. The power evidently drops near 1.5 mHz which is consistent with expected p-mode properties for Procyon. If we assume that the noise is flat around 1 mHz the amplitude of the strongest peak can be estimated, according to the same method as described above, to about 0.50–0.60 ms^{-1}. The power spectrum of η Cas (Fig. 7) shows that the noise in our data can be considered as white (i.e., flat) above 0.5 mHz. As this can not be absolutely true for Procyon observations we made several simulations with noise consistent with actual data. We first simulated the time series with two noise components as described in Kjeldsen & Bedding (1995). The amplitude in a low frequency band was obtained by fitting the power spectra by 1/f noise-component and the amplitude of the random noise was derived from $\sigma_{\mathrm{hf\_ps}}$ for each night.

The resulting power spectra of the time sequences containing only noise and sampled through the same window function as the observations is shown on the left bottom panel of the Figure 8. We performed then the simulations with an artificial oscillating signal containing 3 sets of frequencies equally spaced within a broad solar-like envelope centered at 1 mHz and with a maximum amplitude of 50 cms^{-1} as deduced from the observations. The right top panel of the Figure 8 illustrates the power spectrum

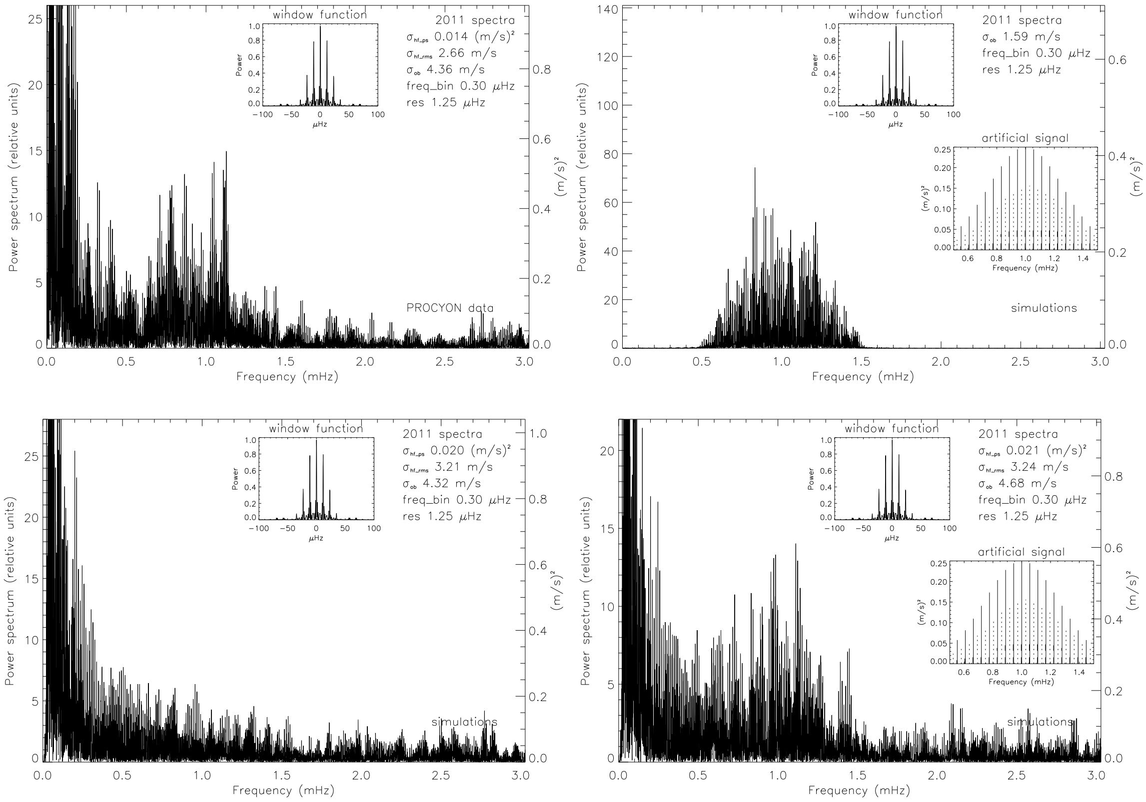

Fig. 8. Left top panel : Power spectrum of Doppler shift measurements (8 nights) for Procyon. Right top panel : Power spectrum of a simulated oscillations data set (shown in the bottom inset) with no noise. Left bottom panel : Power spectrum of simulated noise (white noise and 1/f noise extrapolated from the observations). Right bottom panel : Power spectrum of the artificial signal in presence of noise. The generated signals have exactly the same sampling function as the observations. The common inset shows the power spectrum of the window function for a signal amplitude of $1\,\mathrm{ms}^{-1}$ and the same sampling rate as the observations.

of one simulated oscillation data set, the modes and their respective amplitudes are shown in the inset of the figure.

More extensive simulations of the synthetic oscillation spectra obtained from p-mode frequencies calculations using the stellar models for Procyon are presented in Barban et al.(1999). Finally, the power spectrum of the simulated time series with an artificial signal in presence of noise and with a rms almost equal to that in observed data is shown in the right bottom panel of the Figure 8. Although the noise in the simulated time sequences is probably overestimated due to the fitting process described above, it is still possible to see the hump of excess power between 0.5 and 1.5 mHz introduced by the injected signal with maximum amplitude of $50\,\mathrm{cms}^{-1}$.

By comparing actual data and simulations we can explain the irregular shape of the excess power by constructive interference between modes (Brown & Gilliland 1990, Barban et al. 1999) or/and by constructive interference with noise peaks. During particular realization of the two simulations without noise and with noise shown on the right top and bottom panels of the Figure 8 we kept the same set of phases (randomly distributed) and amplitudes of oscillation modes. The amplitudes of the largest peaks around 1 mHz in the second simulation are then strengthened only by interference with randomly distributed noise peaks. All these interferences and important sidelobes due to daily aliases make the identification of the modes difficult (see next section).

5. Results of CLEAN analysis

The asymptotic relation, first developed by Tassoul (1980), for modes with radial order n much greater than l predicts a series of oscillation frequencies with almost uniform separation usually defined as the large frequency splitting ($\Delta\nu_0$). In the search for solar-like oscillations, a classical way to support the detection of a stellar signal is to search for the quasi-equidistant set of peaks within the frequency range of hump of excess power. One technique commonly used to determine the first order spacing $\Delta\nu_0$ is to calculate the "comb response" of the power spectrum (Kjeldsen et al. 1995). If the power spectrum includes peaks having regular spacing from the largest peak assumed to be the oscillation mode, then the frequency

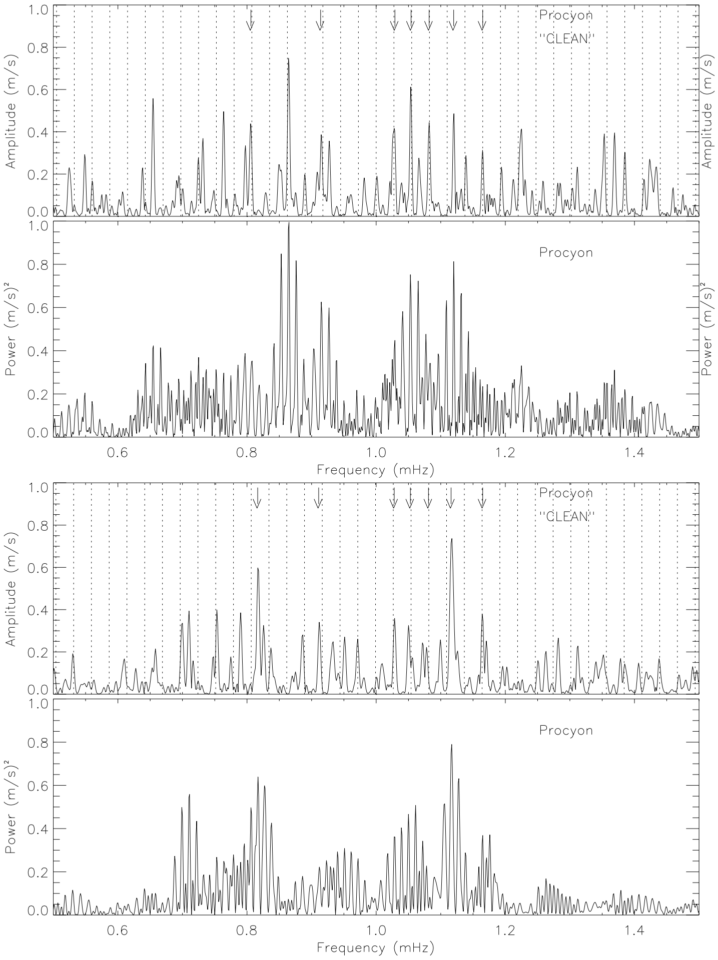

Fig. 9. Top panel : Power and CLEANed spectra of the Doppler shift of the four first nights (Nov 7-10, 1998).
Bottom panel : Power and CLEANed spectra of the Doppler shift of the three last nights (Nov 14-16, 1998). The dashed lines indicate frequencies equal to $\Delta\nu_0(n+l/2)$, $\Delta\nu_0 = 55\,\mu$Hz, $n=[12,24], l=[0,1]$

of the maximum peak of the comb function will be the searched value of frequency splitting.

We first applied the comb response to two periodograms of the first four and three last nights of Procyon observations. Because of the sidelobes of substantial amplitude due to daily gaps in the power spectrum, we obtained no clear comb function signature. Consequently, in order to remove the effects of the window function, we processed our two independent time series with the "CLEAN" procedure (Roberts et al. 1987). The data of each night have been high-pass filtered below 0.3 mHz in order to attenuate the power at the lowest frequencies, in particular, from the first nights. We checked that the filtering process does not alter the positions of peaks in the interval of excess power.

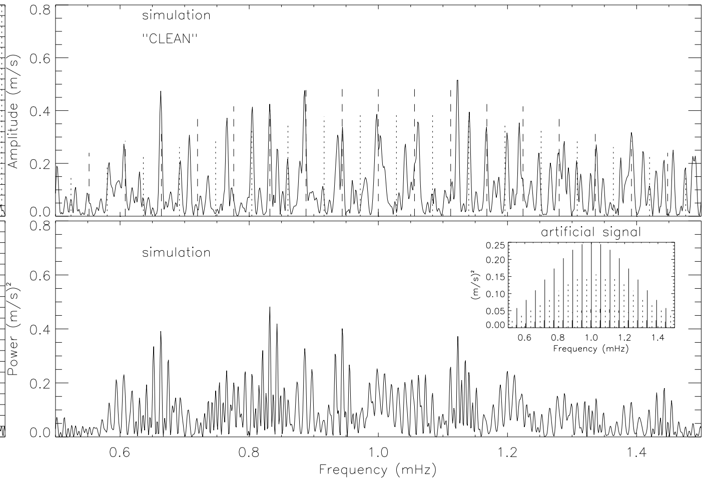

Fig. 10. Bottom panel : Power spectrum of an artificial signal (visible in the inset) plus white noise, calculated with the same observational window as the last 3 nights of observation.
Top panel : Resulting CLEANed spectrum. The dashed lines indicate the two sets of frequencies of the injected signal.

In Fig. 9, one may compare the periodogram and the CLEANed spectrum of each time series in the frequency range of excess power. The CLEAN algorithm works well enough, the amplitudes of the sidelobes are clearly reduced and most of the large peaks stay at the same place as on the periodograms. Here, we note only the frequencies of maximum of peaks (those with power greater than $0.3\,(\mathrm{ms}^{-1})^2$) that are common ($\pm 5\,\mu$Hz) between 0.6 mHz and 1.4 mHz in the two clean spectra. We note also the first-order frequency spacing from the comb response computed at these frequencies :

First data set (4 consecutive nights) :
ν (mHz) : 0.806, 0.914, 1.029, 1.054, 1.082, 1.120, 1.165
$\Delta\nu$ (μHz) 55.6, 53. , 55.3, 54.9, 56., 55., 55.6
Second data set (3 consecutive nights) :
ν (mHz) : 0.816, 0.911, 1.028, 1.053, 1.081, 1.116, 1.165
$\Delta\nu$ (μHz) 57., 56.7, 58., 54.5, 55.4, 52., 57.2

Taking into account the frequency resolution of respectively $3.56\,\mu$Hz and $5.07\,\mu$Hz for the two time series, the identification of individual modes in clean spectra (oversampled by 4) is subjected to great caution.

For example, in both the periodogram and the CLEANed spectrum of the artificial time series (see Fig. 10), the gaps and noise shift the peaks from the original frequencies or reinforce one peak by mixing multiple frequencies. Moreover, in the CLEANed amplitude spectrum obtained from the simulations with a frequency resolution of the second data set, some of the peaks are double or too wide to allow an unambiguous determination

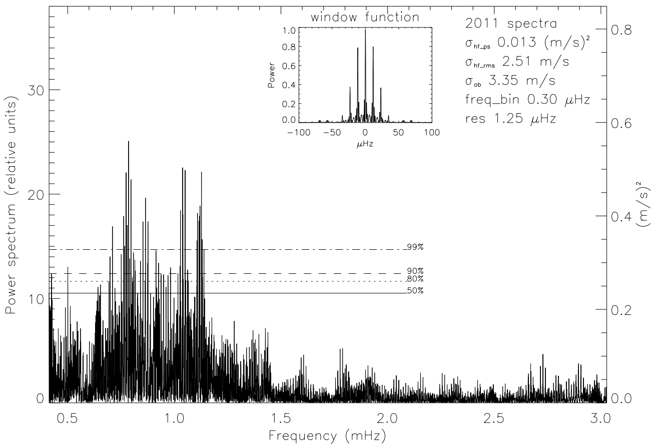

Fig. 11. Power spectrum of the eight-night time-series of the Doppler shift measurements for Procyon, filtered below 0.3 mHz. The inset shows the power spectrum of the window function of the observations, for a signal amplitude of $1\,\mathrm{ms}^{-1}$.

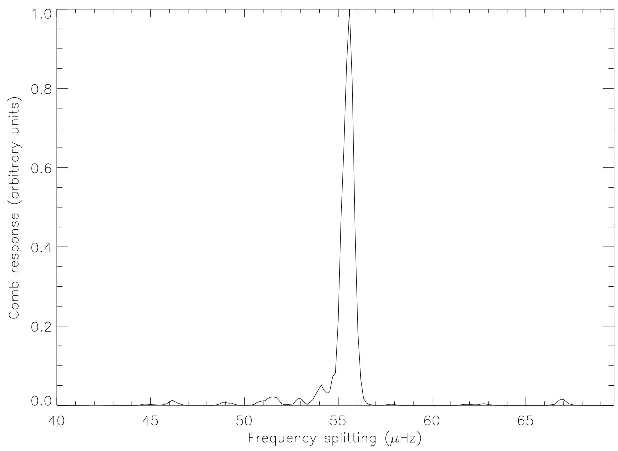

Fig. 12. Example of Comb response of the CLEANed power spectrum of Procyon Doppler shift computed with $0.3\,\mu$Hz resolution from 8 nights of observations.

of the mode frequencies. Nevertheless, we calculated the shift of the individual peaks in the CLEANed spectra of the two observational data sets with respect to the regular grid with different spacings found by comb response. The smallest average shift was obtained using a regular grid with spacing $\Delta\nu_0 = 55\,\mu$Hz (indicated by dashed lines in the Fig. 9). This value for the large frequency spacing can be compared to $\Delta\nu_0 = 53\,\mu$Hz found by Mosser et al. (1998).

Fig. 11 shows the power spectrum of the whole sequence of 8 nights of Procyon, filtered below 0.3 mHz. For five significant peaks, we calculated the mean "true" power level and found a mean amplitude of about $0.47\,\mathrm{ms}^{-1}$ in the 0.6–1.5 mHz frequency range.

Fig. 12 shows one comb response calculated at the frequency 1.065 mHz in the CLEANed power spectrum (not presented here) of Fig. 11. More detailed cleaning of the power spectrum of the entire run (2022 spectra) interrupted by two large gaps of 42 hours is needed to identify with higher precision the oscillation mode frequencies on Procyon.

6. Discussion

The analysis of the time series of Doppler shifts described above has revealed the presence of a strong concentration of power around 1 mHz, which is likely to be due to solar-like p-modes on Procyon. The estimation of the amplitude of the oscillations is of the order of $50\,\mathrm{cms}^{-1}$ which is below predicted amplitudes by Houdek et al. (1995). The most probable frequency spacing is about 55 μHz while the frequency cutoff is around 1.5 mHz. This characteristic frequency spacing is consistent with theoretical predictions for Procyon A (see, e.g, Guenther & Demarque 1993, Barban et al. 1999).

We have also presented a preliminary identification of the p-mode frequencies of Procyon. Several modes seem to be found in both data sets constructed from adjacent nights, but more detailed cleaning (e.g. using the CLEANest algorithm, Foster 1995) is needed, especially for a whole run (complicated window function) to unambiguously confirm the mode detection. Although several peaks are recurrent on individual spectra and the average power spectrum shows an excess of power, a typical "picket-fence" effect in solar-oscillations spectrum is not observed. This can be explained by interferences with noise or/and between modes through the observational window.

Rather severe conclusions by Kjeldsen & Bedding (1995) based on their simulations of noise spectra cast serious doubts on all existing claims of p-mode detection on solar-like stars. However the challenge to show the results, even if doubts persist, is great, since there is always the possibility of confirmation by future independent observations. Our observations confirm the excess of power found by Brown et al. (1991) in the 0.5–1.5 mHz range. In the case of the Brown et al. measurements, Kjeldsen & Bedding were able to reproduce the overall shape of the observed power spectrum of Procyon with two noise components model only and using the same high-pass filter. In our case, one can exclude any influence of high-pass filtering. On the other hand, one can always suspect some unknown noise effect producing a power excess in the p-mode frequency range of Procyon. We verified that the instrumental noise, given by simultaneous Fabry-Perot recordings, do not present any kind of narrow band feature in the power spectrum.

Moreover, the results obtained with the η Cas observed in almost identical night conditions and with the same window function like Procyon's first data set (4 consecutive nights) show a flat spectrum in the 0.6–1.5 mHz interval. Note that from this observing run on η Cas, we obtained the limit of about 30 cms^{-1} for the detection of 5-min oscillations. As emphasized by Peri (1995), η Cas is the most promising candidate in the northern hemisphere for the detection of solar-type oscillations. It was effectively a difficult choice for us, taking into account a limited number of allocated nights for asteroseismology, to observe Procyon for the rest of the night rather than η Cas. Since the primary objective is to have the best temporal coverage as possible in order to identify the p-modes, the seeing conditions favored the brighter star Procyon with higher expected amplitude oscillations. In conclusion, we expect to confirm the results presented in this paper from future multisite observations using the instruments of comparable sensitivity.

Acknowledgements. Without the help of the OHP technical staff, this work would not have been possible. We thank G. Adrianzyk, G. Knispel, D. Kohler, J.-P. Meunier, A. Vin for their invaluable on site support. We are also indebted to G. Rau for his assistance during the observations. It is a pleasure to acknowledge the efficient help of the OHP directors A. Labyerie and J.P. Sivan. One of us (MM) is grateful to D. Queloz and L. Weber for their help in using and modifying ELODIE software at the very beginning of our runs. MM and JCL thank D.H. Roberts for sending us his CLEAN algorithm. We thank the referee, F. Varadi for extensive comments on a first version of the paper. We acknowledge INSU in the frame of Action Incitative 1994 and Observatoire de Paris for the financial support.

References

Ando, H., Watanabe E., Yutani, M., Shimizu, Y. and Nishimura, S., 1988, PASJ 40, 249
Baranne, A., Queloz, D., Mayor, M. et al., 1996, A&AS 119, 373
Barban, C., Michel, E., Martic, M.,Schmitt, J.,Lebrun, J-C., Baglin, A.,Bertaux, J-L., 1999, A&A, submitted
Bedford, D.K., Chaplin, W.J., Coates, A.R., Innis, J.L., Isaak, G.R. and Speake, C.C., 1995, MNRAS 273, 367
Brown, T.M. et al., 1998, in Proc IAU colloquium 170; Precise stellar radial velocities, ed. J.B. Hearnshaw and C.D. Scarfe, Conference series ASP, to be published
Brown, T.M., Noyes, R.W., Nisenson, P., Korzennik, S.G. and Horner, S., 1994, PASP 106, 1285
Brown, T.M., Gilliland, R.L, Noyes, R.W. and Ramsey, L.W., 1991, ApJ 368, 599
Brown, T.M. & Gilliland, R.L, 1990, ApJ 350, 839
Chaboyer, B., Demarque, P., Gentler, D.B, 1998, in: A half-Century of Stellar Pulsation Interpretations: A tribute to Arthur N. Cox, Bradley P.A., Guzik J.A. (eds), ASP Conf. Series, Vol 135, 67
Connes, P., 1978, in: Workshop on Extrasolar Planetray Detection, NASA publ. 2124, 197
Connes, P., 1985, Ap&SS 110, 211
Connes, P., Martic, M. and Schmitt, J., 1996, Ap&SS 241, 61
Edmonds, P.D. & Cram L.E., 1995, MNRAS 276, 1295
Foster, G., 1995, AJ 109(4), 1889
Gelly, B., Grec, G., Fossat, E., 1986, A&A 164, 383
Girard, T.M, Wu, H., Lee, J.T., Dyson, S.E., 1996, BAAS 28, 919
Gilliland, R.L. et al., 1993, AJ 106, 2441
Guenther, D.B. & Demarque P., 1993, ApJ 405, 298
Horn, K., 1986, PASP 98, 609
Horne, J.H., Baliunas, S.L, 1986, ApJ 302, 757
Houdek, G., Rogl. JH., Balmforth N.J., and Christensen-Dalsgaard J., 1995, In "GONG 94: Helioseismology and Asteroseismology", R.K Ulrich, E.J Rhodes, and Dappen, Eds., ASP Conference Seies, Vol 76, 641
Hoyng, P. , 1976, A&A 47, 449
Kjeldsen, H., Bedding, T., Viskum, M., Frandsen, S., 1995, AJ 109(3), 1313
Kjeldsen, H. & Bedding, T., 1995, A&A 293, 87
Lomb, N.R., 1976, Ap&SS 39, 447
Innis, J.L., Isaak, G.R., Speake, C.C., Brazier, R.I., Williams, H.K, 1991, MNRAS 249, 643
Irwin, A.W, Fletcher, J.M, Yang, S.L.S, Walker, G.A., Goodenough, Ch., 1992, PASP 104, 489
Mayor, M. & Queloz, D., 1995, Nature 378, 355
Mosser B., Maillard J.P., Mékarnia D., and Gay J., 1998, A&A 340, 457
Peri, M.L, 1995, Ph. D Thesis
Pottasch, E.M., Butcher, H.R. and van Hoesel, F.H.J., 1992, A&A 264, 138
Roberts, D.H., Léhar, J. and Dreher, J.W., 1987, AJ 93(4), 968
Scargle, J.D., 1982, ApJ 263, 835
Tassoul, M., 1980, ApJ&S 43, 469
Young, A. and Rottler, L., 1992, PASP, 104, 71